Improvement to the gross theory of β decay by inclusion of change in parity

Hiroyuki Koura*
Advanced Science Research Center, Japan Atomic Energy Agency, Ibaraki 319-1195, Japan

Satoshi Chiba
Laboratory for Advanced Nuclear Energy, Institute of Innovative Research, Tokyo Institute of Technology, Ookayama, Tokyo 152-8550, Japan
(Received 6 December 2016; published 5 June 2017)

An improvement to the single-particle structure is made to the gross theory, which is a global β-decay model. The gross theory is based on the sum rule of the intensity of the β-decay transition and a strength function. This model provides reasonable results for β-decay rates and delayed neutrons for the entire nuclear mass region. An attempt is made to improve the gross theory of nuclear β decay by considering the change in parity at the single-particle level of ground-state nuclei. In this treatment, the nuclear matrix elements are suppressed when the parity of the single neutron and proton levels is different for the allowed transition. The assignment of parity is performed using the Woods-Saxon–type single-particle potential. The discrepancies from experimental half-lives, which appeared in the vicinity of the magic numbers of neutrons and protons, are systematically improved in the nuclear mass region.

DOI: 10.1103/PhysRevC.95.064304

I. INTRODUCTION

β decay occurs due to the weak interaction, and a nucleus in a neutron-rich nuclear mass region releases an electron, a γ ray, and an antineutrino. The β^- decay process occurs in neutron-rich nuclei and plays an important role in nuclear astrophysics, such as in the r-process nucleosynthesis in stars or when manipulating a nuclear reactor with delayed neutrons, which are emitted in an accompanying process. In order to theoretically estimate the β-decay rate and the delayed neutron probability, it is necessary to calculate the nuclear matrix elements of the β decay. The gross theory is a macroscopic model that describes various types of β decay. The gross theory is based on the sum rule of the β-decay strength function and treats the transitions to all the final nuclear levels in a statistical manner. It has been successful in describing β decay for the entire range of nuclear masses [1–7]. The results obtained by the gross theory provide a guide for experiments on β decay, especially for newly measured nuclear data, such as very-neutron-rich nuclei, and for purely theoretical nuclei that are extremely different from known nuclei. Due to its statistical treatment, the gross theory only describes macroscopic features, and the gross theory ignores microscopic properties such as spin and the parity of nuclei.

In the preset paper, we introduce a microscopic correction to the gross theory and discuss its effect on the half-lives of β decay. In particular, we focus on the parity change when interchanging a ground-state neutron and proton in a single-particle state. We estimate a single-particle state with a global single-particle potential and suppress the allowed transition of the β decay. The essential difference in this model is its treatment of the β-decay strength function, which corresponds to the squared transition matrix element. In Sec. II, we present a short introduction to the theory of β decay. In Secs. III and IV, we review the gross theory and discuss the proposed improvements to the gross theory, respectively. The obtained results and a discussion are presented in Sec. V. Finally, a summary is presented in Sec. VI.

II. BETA DECAY

The decay constant of the β decay is divisible by the β-decay operators, Ω, and it is obtained as the sum of the partial decay constants, λ_Ω. If we take into account the allowed transitions and the first forbidden transition, the total β-decay rate can expressed as

$$\begin{aligned}\lambda_\beta &= \lambda_{\text{allowed}} + \lambda_{\text{first-forbidden}}\\ &= \lambda_{\text{F}} + \lambda_{\text{GT}} + \lambda_1^{(0)} + \lambda_1^{(1)} + \lambda_1^{(2)},\end{aligned} \tag{1}$$

where the terms on the right-hand side are the decay rate of the Fermi transition, the Gamow-Teller transition, and the first-forbidden transitions of rank $L = 0, 1$, and 2, respectively. The type of β decay is determined by the change in the spin-parity between the parent and daughter nuclei.

Under the usual approximation, the decay rate can be written in terms of the nuclear matrix elements, $|M_\Omega(E)|$, which can be calculated in the framework of nuclear physics, and the integrated Fermi function, $f(E)$, which represents the distortion of the wave functions, due to the Coulomb force, as follows:

$$\lambda_{\text{F}} = \frac{m_{\text{e}}^5 c^4}{2\pi^3\hbar^7}|g_{\text{V}}|^2 \int_{-Q_\beta}^{0} |M_{\text{F}}(E)|^2 f(-E)dE,$$

$$\lambda_{\text{GT}} = \frac{m_{\text{e}}^5 c^4}{2\pi^3\hbar^7}|g_{\text{A}}|^2 3 \int_{-Q_\beta}^{0} |M_{\text{GT}}(E)|^2 f(-E)dE,$$

$$\lambda_1^{(2)} = \frac{m_{\text{e}}^5 c^4}{2\pi^3\hbar^7}\left(\frac{m_{\text{e}}c}{\hbar}\right)^2 |g_{\text{A}}|^2 \int_{-Q_\beta}^{0} \sum_{ij} |M_{ij}(E)|^2 f(-E)dE,$$

*koura.hiroyuki@jaea.go.jp

$$\lambda_1^{(1)} = \frac{m_e^5 c^4}{2\pi^3 \hbar^7}\left(\frac{m_e c}{\hbar}\right)^2 \left[|g_V|^2 \int_{-Q_\beta}^{0} |M_{\boldsymbol{r}}(E)|^2 f_{1V}(-E)dE + |g_A|^2 \int_{-Q}^{0} |M_{\boldsymbol{\sigma}\times\boldsymbol{r}}(E)|^2 f_{1A}(-E)dE \right],$$
$$\lambda_1^{(0)} = \frac{m_e^5 c^4}{2\pi^3 \hbar^7}\left(\frac{m_e c}{\hbar}\right)^2 |g_A|^2 \int_{-Q_\beta}^{0} |M_{\boldsymbol{\sigma}\cdot\boldsymbol{r}}(E)|^2 f_{1A}(-E)dE. \quad (2)$$

Here, the coefficients are composed of the coupling constant of the weak interaction and the following physical constants: the mass of the electron, m_e; the speed of light, c; and the reduced Planck constant, $\hbar$. There are two types of coupling constants for the weak interaction: the vector g_V and the axial vector g_A. The integral is performed from $-Q_\beta$ to 0, and Q_β is the total (maximum) decay energy from the ground state of parent-to-daughter nuclei (the β-decay Q value).

The nuclear matrix elements and the integrated Fermi function are necessary in order to calculate the β-decay rate. For the integrated Fermi function, the numerical values can be rather easily and precisely obtained. The calculation of the nuclear matrix elements, however, is rather difficult because of the complexity of the nuclear many-body problem with a complicated nuclear force. Two types of approaches that are applicable to nuclei in the entire mass region have been investigated: microscopic approaches, which include quasiparticle random phase approximation (QRPA) and probably the shell model, and macroscopic approaches, which include the gross theory (GT), which is the focus of the present study and is summarized in Sec. III.

III. GROSS THEORY

The gross theory of β decay assumes that the sum of the intensity remains constant during the transition from the initial state to the final state. Note that β decay also obeys such a sum (and an energy-weighted sum) rule.

In the gross theory, a one-particle strength function, D_Ω, is introduced, and the squared nuclear matrix element can be written as

$$|M(E)_\Omega|^2 = \int_{\epsilon_{\min}}^{\epsilon_{\max}} D_\Omega(E,\epsilon)W(E,\epsilon)\frac{dn_1}{d\epsilon}d\epsilon, \quad (3)$$

where ϵ is the one-particle energy of the decaying nucleons, and E is the (observable) transition energy measured from the parent state. The function $W(E,\epsilon)$ is a weighting function that reflects the Pauli exclusion principle, and $dn_1/d\epsilon$ is the one-particle energy distribution of the decaying nucleons. The one-particle strength function, $D(E,\epsilon)$, is a smooth function, and satisfies the same sum and energy-weighted sum rules as $|M(E)|^2$. For the Fermi transition, the strength function is chosen such that it forms a sharp peak at the energy of the isobaric analog state (IAS), and has a long-tailed distribution over all E. For the Gamow-Teller transition, the strength function is chosen such that it has a peak at a few MeV above the energy of the IAS, and is a broad-tailed distribution. In a

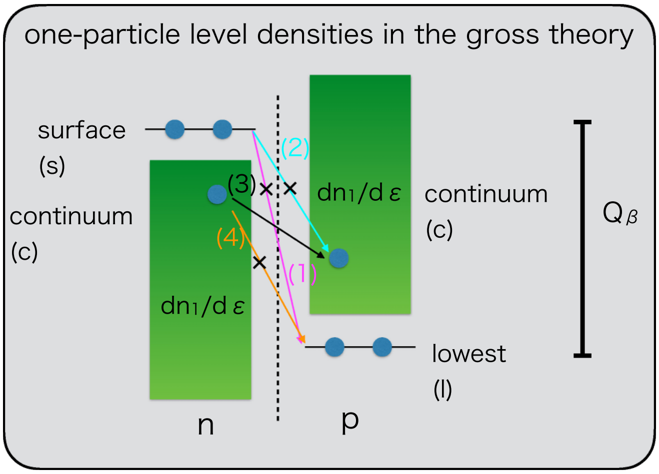

FIG. 1. One-particle level densities: (1) surface to the lowest level, $|M_{\Omega s\to l}|^2$; (2) surface to continuum, $|M_{\Omega s\to c}|^2$; (3) continuum to continuum, $|M_{\Omega c\to c}|^2$; and (4) continuum to the lowest level, $|M_{\Omega c\to l}|^2$.

current study, a combination of hyperbolic-secant functions is adopted as the functional form of $D(E,\epsilon)$ [6].

Nuclear levels are treated as single discrete levels at the Fermi surface and elsewhere as a continuum of levels, according to the Fermi gas model [2], as shown in Fig. 1. The major components of probable transitions can be listed as follows: (1) discrete-to-discrete levels, (2) discrete-to-continuum levels, (3) continuum-to-continuum levels, (4) continuum-to-discrete level, and (5) incoherent transitions. The total squared nuclear matrix element is therefore composed of the following terms:

$$|M_\Omega(E)|^2 = |M_{\Omega s\to l}(E)|^2 + |M_{\Omega s\to c}(E)|^2 + |M_{\Omega c\to c}(E)|^2 + |M_{\Omega c\to l}(E)|^2 + \text{incoherent}. \quad (4)$$

Here, s is the discrete level of the neutron (the surface level), l is the discrete level of the proton (the lowest level), and c is the continuum of levels for the β^- case (see Fig. 1).

In the first component, $|M_{\Omega s\to l}(E)|^2$, the distribution of the matrix element concentrates into the ground state of the daughter nucleus, $E = -Q_\beta$, therefore the cross terms of $M_{\Omega s\to l}(E)$ with other components of the matrix element like $M_{\Omega s\to l}(E)\cdot M_{\Omega s\to c}(E)$ are small or negligible (i.e., no incoherence). In the actual calculation carried out in this study, $|M_{\Omega s\to l}(E)|^2$ is treated as a δ function, $\delta_{-Q_\beta}(E)$ [2]. In the second component, $|M_{\Omega s\to c}(E)|^2$, the distribution of the squared matrix element is described by $D(E,\epsilon)$ [and $W(E,\epsilon)$], and in the third component, $|M_{\Omega c\to c}(E)|^2$, the distribution of the squared matrix element is the integral of the product of the Fermi-gas level densities and $D(E,\epsilon)$ [and also $W(E,\epsilon)$]. In the third component, the absolute value of the squared matrix element near the ground state of the daughter nucleus at $E = -Q$ is small due to the small value of $dn_1/d\epsilon$ at these energies. Therefore, the cross terms of the matrix elements with $M_{\Omega c\to c}(E)$ in the lower E region are expected to be small. However, in the higher energy region, these cross terms seem to be large. Concerning the decay rate, a large number of decay transitions are located near the ground state of the daughter

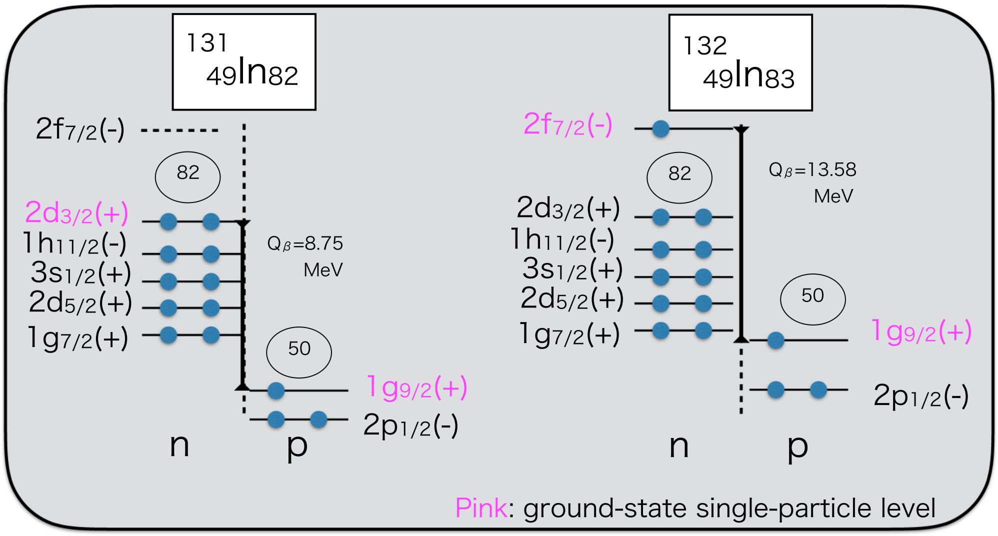

FIG. 2. Schematic diagram of single-particle levels for ${}^{131}_{49}\mathrm{In}_{82}$ and ${}^{132}_{49}\mathrm{In}_{83}$. (n: neutron, p: proton.) The text in pink indicates the ground-state level. The indicated levels were estimated from data presented in Ref. [9].

nucleus due to $f(E)$ being generally large near this region on a logarithmic scale. In the fourth component, $|M_{\Omega c\to 1}(E)|^2$, we could give a similar discussion to the third component.

Based on the above discussion, although the contribution of the incoherent components to the total squared nuclear matrix element might be expected not to be small, we assume that incoherent components can be omitted. Thus, in the following, we discuss transitions only in terms of the first four components. The interference terms may affect the results of the gross theory in more precise analysis, and we will study the influence of the interference terms to the gross theory in the near future.

Equation (4) holds for even-even nuclei. For other cases, such as odd-A and odd-odd nuclei, the treatment of the discrete levels is more complicated and some correspondent components are added. However, Eq. (4) remains as a main component. For details, see Ref. [2]. In another study, a BCS-type pairing configuration was phenomenologically introduced [5].

In the gross theory, the first-forbidden transition and the allowed transition were taken from an earlier study [3]. The resulting form is shown as Eq. (1). The first version of the gross theory (GT1) is given in Ref. [4], and the second version of the gross theory (GT2) is given in Ref. [7].

The β-decay half-lives calculated using the gross theory generally exhibit a smoother trend on the isotopic systematics for the entire region of the nuclei, as compared to “microscopic” models. In some cases, the half-lives calculated by the gross theory are consistent with experimental trends, and an example of this is shown for neutron-rich nuclei in Ref. [8].

IV. IMPROVEMENTS TO THE GROSS THEORY

The decay constant for β decay is expressed as in Eq. (1). Note that each transition depends on the particular nuclear structure, such as the spin, parity, and deformation. In the framework of the original gross theory, the transitions are not restricted by the nuclear microscopic properties. The intensities of all transition types are calculated for the corresponding E, and, for all nuclei, they are integrated from $-Q_\beta$ to 0.

Consider a single-particle level for the neutron and proton in the ground state at a Fermi surface. Figure 2 shows examples of this situation for ${}^{131}_{49}\mathrm{In}_{82}$ and ${}^{132}_{49}\mathrm{In}_{83}$. In the case of ${}^{131}_{49}\mathrm{In}_{82}$, the single-neutron level of the ground state is $2d_{3/2}$ with positive parity, while the single-proton level of the ground state is $1g_{9/2}$ with positive parity. Note that these levels have the same parity. In the case of ${}^{132}_{49}\mathrm{In}_{83}$, however, the single-neutron level of the ground state changes to $2f_{7/2}$ with negative parity, and this change affects the transition. In an actual nucleus undergoing β decay, the decay rate is the sum of all of the corresponding transitions at all possible levels between neutrons and protons. However, the ground-to-ground state transition is generally dominant, because the integrated Fermi function, $f(E)$, at the ground state of the daughter nucleus is generally large on a logarithmic scale.

In general, an allowed transition should be forbidden if the parities of the parent and daughter nuclei are different and if the change in spin is greater than one. Considering the above situation, we add a factor to the gross theory to hinder particular transitions, especially allowed transitions. Although such a selection rule must be obeyed in order to modify the model, in the original gross theory, the decay rates are treated as a simple sum independent of the single-particle states. In the case of ${}^{131}_{49}\mathrm{In}_{82}$, the actual transition between the ground-state neutron and proton levels is the second forbidden transition; however, the gross theory gives the half-life of this nucleus in terms of the sum of the allowed and the first transition rates. Furthermore, in the current framework of the gross theory, the levels are on a continuum, so the realistic spin-parity of nuclei cannot be considered. We will thus make some assumptions and refine the theory as described below.

The squared matrix element is expressed as shown in Eq. (4). The discrete levels (l and s) correspond to the

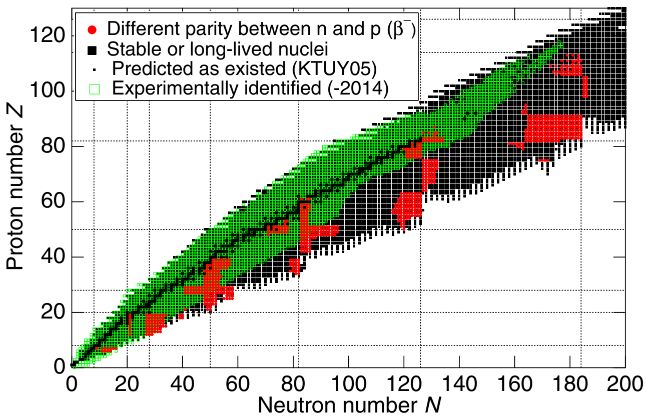

FIG. 3. Mismatching of parity between ground-state neutron levels and proton levels (red). Only nuclei on the β^- side are plotted. Filled squares (black): stable or long-lived nuclides. Open squares (green): nuclides experimentally identified [11]. Dots (gray): nuclides predicted to exist by the KTUY mass model [10].

ground-state levels. The continuum (c) includes levels with various types of spin-parity. Therefore, we propose a model to estimate the spin-parity of both single-neutron and single-proton ground-state levels, where the matrix elements related to these discrete levels contain a hindrance. When the parity of the ground-state neutron and proton are mismatched in the allowed transition, in the model calculations, the matrix-element parts, s → l, l → c, and c → l, are eliminated, and the continuum-to-continuum part, c → c, remains, as shown in Fig. 1. In our phenomenological approach, we focus only on parity mismatching, and the change in spin is not further considered in this study.

Note that this treatment is applied to all nuclei, i.e., even-even, odd-A, and odd-odd nuclei. In the case of odd-A, the estimated spin-parity may coincide with what is found experimentally, if the total experimental spin-parity is governed by the single-particle state.

In order to estimate the spin-parity, we adopt a modified Woods-Saxon potential for spherical nuclei over the entire nuclear chart [9]. This only applies to small nuclear shapes. We estimate the nuclear deformation from a global calculation of ground-state nuclear masses and then apply the KTUY mass formula [10] to the estimation. The threshold deformation parameter is determined so that experimental trends are reproduced, and we adopt the parameter $\alpha_2 = 0.05$.

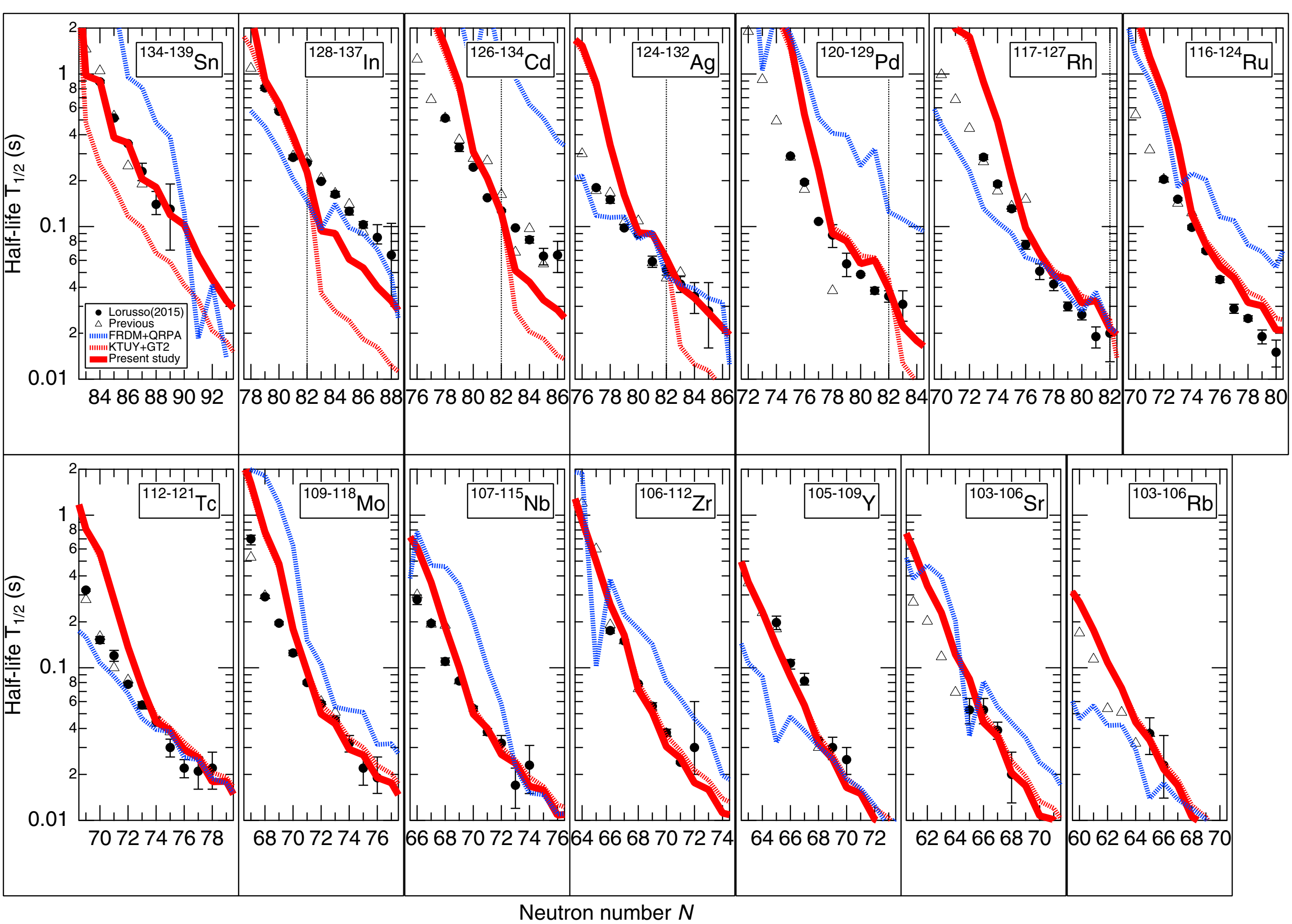

FIG. 4. β^--decay half-lives for rubidium to tin isotopes in the neutron-rich mass region. Dashed red line: results of the original gross theory. Thick solid red line: results of the improved gross theory. Blue dashed line: FRDM+QRPA [12]. Open triangles: data from experiments reported prior to 2015. Solid circles: experiment results reported in 2015 [13].

Figure 3 shows the locations of mismatched parity for a wide region of nuclear masses. The region with mismatching is located near points that result in the magic numbers of neutrons and protons (for example, $N \sim 126$ with $60 \leqslant Z \leqslant 80$, and $N \sim 82$ with $40 \leqslant Z \leqslant 60$). The region in which $N > 82$ with $Z \approx 50$ corresponds to a parity-mismatching combination of $2f_{7/2}(-)$ for the neutron level and $1g_{9/2}(+)$ for the proton level, as shown in Fig. 2. Other cases are given in the same manner.

V. RESULTS

Figure 4 shows the β^--decay half-lives for rubidium ($Z = 37$) to tin ($Z = 50$) isotopes in the neutron-rich mass region. In the region above $N = 82$, the half-lives obtained from the original gross theory [7] with the KTUY mass model [10] (thin line) systematically slope downward and underestimate the experimentally measured values. These isotopes are located in the mismatched region shown in Fig. 3. At $N = 82$, the β-decay Q value changes sharply, and the half-lives calculated using the original gross theory follow the trend of Q-value systematics and exhibit a steep down slope as N increases. The improved gross theory (thick lines) increases the half-lives in this region, and consequently the slope is more gradual. This follows the trend observed in experimental data. The main component determining the half-life comes from the remaining continuum-to-continuum part of Eq. (4). The first-forbidden component provides a minor contribution to the half-life of these nuclei. The results of the FRDM + QRPA calculation [12] are also plotted, and these results diverge from the experimental data and sometimes exhibit a kink.

Figure 5 shows the ratio between the theoretical and experimental half-lives on a logarithmic scale. In the initial gross theory (upper panel), underestimated regions are located near the magic numbers: $Z \approx 50$ with $N \approx 82$, $N > 50$ around $Z \approx 38$, $Z \approx 20$ with $N \approx 28$, and so on. In the improved gross theory (lower panel), these periodic underestimations weaken or disappear, and in their place, there are more overestimated regions, such as $Z \approx 28$ with $40 < N < 50$.

Table I shows examples of experimental and calculated β-decay half-lives for selected nuclei. In the case of $Z = 18$ with $N = 28$–32 and $Z = 36$ with $N = 54$–56, the improved half-lives ('present study' in the table) become longer and are generally comparable to the experimental results. In the case of $Z = 49$ with $N = 82$–84, the improvement appears to be insufficient. However, the trend is somewhat better than for previous studies, as shown in Fig. 4. The case of $Z = 28$ isotopes in the vicinity of ^{78}Ni in the original gross theory provides excellent results, whereas the improved calculation provides worse results.

Note again that, in the case of (49, 82), $^{131}_{49}\mathrm{In}_{82}$, the calculation is still performed using the sum of the allowed transition and the first-forbidden transition given by Eq. (1), although the transition is actually a second-forbidden transition considered from the ground-state configuration in spin-parity.

In the present study, we treat only a suppression of the allowed transition on the parity change, and the angular-momentum mismatch is not considered. Therefore the selection rule for the type of β decay has not been actually applied

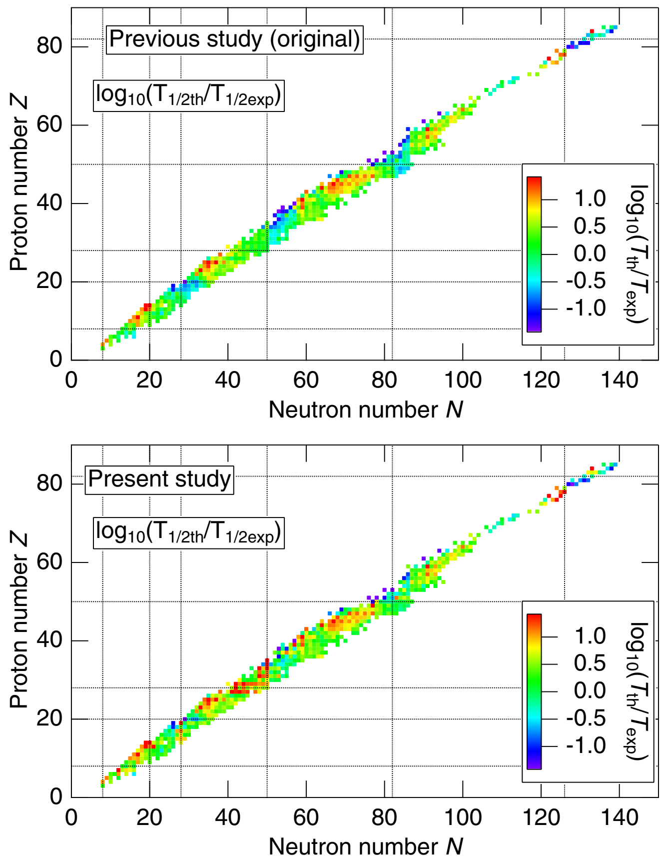

FIG. 5. Ratio of calculated to experimental β^- decay half-lives shown on a logarithmic scale. (Top) The original gross theory. (Bottom) Improved gross theory.

to each nucleus in this framework, i.e., the second-forbidden transition occurs with no parity change, while the calculation

TABLE I. Experimental and calculated β-decay half-lives for selected nuclei. 'Spin-orbit and parity' (second and third column) is the single-proton and -neutron spin-parity at the Fermi surface in the modified Woods-Saxon potential in Ref. [9].

(Z, N)	Spin-orbit and parity		Half-lives (s)		
	proton	neutron	previous	present study	exp. [14]
(18, 28)	$1d_{3/2}(+)$	$1f_{7/2}(-)$	1.04	14.7	8.4
(18, 29)	$1d_{3/2}(+)$	$2p_{3/2}(-)$	0.18	0.35	1.23
(18, 30)	$1d_{3/2}(+)$	$2p_{3/2}(-)$	0.086	0.48	0.47
(18, 31)	$1d_{3/2}(+)$	$2p_{3/2}(-)$	0.050	0.11	0.17
(28, 47)	$1f_{7/2}(-)$	$1g_{9/2}(+)$	0.35	0.67	0.344
(28, 48)	$1f_{7/2}(-)$	$1g_{9/2}(+)$	0.20	0.85	0.238
(28, 49)	$1f_{7/2}(-)$	$1g_{9/2}(+)$	0.14	0.30	0.128
(28, 50)	$1f_{7/2}(-)$	$1g_{9/2}(+)$	0.087	0.32	0.110
(36, 54)	$3p_{3/2}(-)$	$2d_{5/2}(+)$	4.2	28.1	32.22
(36, 55)	$3p_{3/2}(-)$	$2d_{5/2}(+)$	1.5	2.4	8.57
(36, 56)	$3p_{3/2}(-)$	$2d_{5/2}(+)$	0.80	3.9	1.84
(49, 82)	$1g_{9/2}(+)$	$2d_{3/2}(+)$	0.23	(same)	0.28
(49, 83)	$1g_{9/2}(+)$	$2f_{7/2}(-)$	0.037	0.093	0.207
(49, 84)	$1g_{9/2}(+)$	$2f_{7/2}(-)$	0.028	0.090	0.165

here gives no hinderance for it. Further analysis of this improvement is needed.

The gross theory is a global model and considers only the bulk properties of nuclear β-decay transition. The approach proposed herein would improve this model.

In these calculations, we simply suppress the allowed transitions, and, therefore, the sum of intensities of the allowed transitions over the entire energy range may be lower than expected due to the sum rule for corresponding nuclei. This is another area for further study.

VI. SUMMARY

In conclusion, we improved the gross theory of β decay by considering parity changes in the allowed transitions. In this treatment, the nuclear matrix elements are suppressed when the parity of the single neutron and proton are different in the allowed transition. The parity is assigned using the Woods-Saxon–type single-particle potential and the KTUY nuclear mass model. Compared to the experimental data, the original gross theory underestimates the half-lives in the vicinity of the magic numbers of neutrons and protons. This was a result of the proposed improvement.

ACKNOWLEDGMENTS

The present study was conducted as part of the "Comprehensive study of delayed-neutron yields for accurate evaluation of kinetics of high-burn up reactors" program of the Tokyo Institute of Technology and the Ministry of Education, Culture, Sports, Science, and Technology of Japan (MEXT).

[1] K. Takahashi and M. Yamada, Prog. Theor. Phys. **41**, 1470 (1969).
[2] S. Koyama, K. Takahashi, and M. Yamada, Prog. Theor. Phys. **44**, 663 (1970).
[3] K. Takahashi, Prog. Theor. Phys. **45**, 1466 (1971).
[4] K. Takahashi, M. Yamada, and T. Kondoh, At. Data Nucl. Data Tables **12**, 101 (1973).
[5] T. Kondoh, T. Tachibana, and M. Yamada, Prog. Theor. Phys. **74**, 708 (1985).
[6] T. Tachibana, M. Yamada, and Y. Yoshida, Prog. Theor. Phys. **84**, 641 (1990).
[7] T. Tachibana and M. Yamada, *Proceedings of the Inernational Conference on Exotic Nuclei and Atomic Masses, ENAM95* (Editions Frontueres, Gif-sur-Yvette, 1995), p. 763, and references therein.
[8] S. Nishimura, Z. Li, H. Watanabe, K. Yoshinaga, T. Sumikama, T. Tachibana, K. Yamaguchi, M. Kurata-Nishimura, G. Lorusso, Y. Miyashita, A. Odahara, H. Baba, J. S. Berryman, N. Blasi, A. Bracco, F. Camera, J. Chiba, P. Doornenbal, S. Go, T. Hashimoto, S. Hayakawa, C. Hinke, E. Ideguchi, T. Isobe, Y. Ito, D. G. Jenkins, Y. Kawada, N. Kobayashi, Y. Kondo, R. Krucken, S. Kubono, T. Nakano, H. J. Ong, S. Ota, Z. Podolyak, H. Sakurai, H. Scheit, K. Steiger, D. Steppenbeck, K. Sugimoto, S. Takano, A. Takashima, K. Tajiri, T. Teranishi, Y. Wakabayashi, P. M. Walker, O. Wieland, and H. Yamaguchi, Phys. Rev. Lett. **106**, 052502 (2011).
[9] H. Koura and M. Yamada, Nucl. Phys. A **671**, 96 (2000).
[10] H. Koura, T. Tachibana, M. Uno, and M. Yamada, Prog. Theor. Phys. **113**, 305 (2005).
[11] H. Koura, J. Katakura, T. Tachibana, and F. Minato, Chart of the Nuclides 2014, Japanese Nuclear Data Committee and Nuclear Data Center, Japan Atomic Energy Agency (2015).
[12] P. Möller, J. R. Nix, and K.-L. Kratz, At. Data Nucl. Data Tables **66**, 131 (1997).
[13] G. Lurusso *et al.*, Phys. Rev. Lett. **114**, 192501 (2015).
[14] Evaluated Nuclear Structure Data File (ENSDF), Aug. 2014 version, communicated through Nuclear Data Center, Japan Atomic Energy Agency.